Published October 1, 1981

Tetrodotoxin Block of Sodium Channels in Rabbit Purkinje Fibers

Interactions between Toxin Binding and Channel Gating

CHARLES J. COHEN, BRUCE P. BEAN, THOMAS J. COLATSKY, and RICHARD W. TSIEN

From the Department of Physiology, Yale University School of Medicine, New Haven, Connecticut 06510. Dr. Colatsky's present address is Department of Physiology, Cornell Medical College, New York, New York 10021.

ABSTRACT Tetrodotoxin (TTX) block of cardiac sodium channels was studied in rabbit Purkinje fibers using a two-microelectrode voltage clamp to measure sodium current. I_{Na} decreases with TTX as if one toxin molecule blocks one channel with a dissociation constant $K_D \cong 1$ μM. K_D remains unchanged when I_{Na} is partially inactivated by steady depolarization. Thus, TTX binding and channel inactivation are independent at equilibrium. Interactions between toxin binding and gating were revealed, however, by kinetic behavior that depends on *rates* of equilibration. For example, frequent suprathreshold pulses produce extra use-dependent block beyond the tonic block seen with widely spaced stimuli. Such lingering aftereffects of depolarization were characterized by double-pulse experiments. The extra block decays slowly enough ($\tau \cong 5$ s) to be easily separated from normal recovery from inactivation ($\tau < 0.2$ s at 18°C). The amount of extra block increases to a saturating level with conditioning depolarizations that produce inactivation without detectable activation. Stronger depolarizations that clearly open channels give the same final level of extra block, but its development includes a fast phase whose voltage- and time-dependence resemble channel activation. Thus, TTX block and channel gating are not independent, as believed for nerve. Kinetically, TTX resembles local anesthetics, but its affinity remains unchanged during maintained depolarization. On this last point, comparison of our I_{Na} results and earlier upstroke velocity ($\dot{V}_{max}$) measurements illustrates how much these approaches can differ.

INTRODUCTION

Progress toward a molecular understanding of sodium channels has been greatly aided by agents such as tetrodotoxin (TTX) and local anesthetics, which directly interfere with ion permeation. In nerve and skeletal muscle where I_{Na} is most easily studied, block of sodium channels by TTX is strikingly

different from block by local anesthetics. TTX seems to occlude the ion-selective outer mouth of the Na pore without interacting with the gating mechanism (see Hille [1970]; Narahashi [1974]; Ulbricht [1977] for reviews). The neurotoxin has no effect on the time-course of the sodium ionic current (Takata et al., 1966; Hille, 1968) or the magnitude or time-course of the sodium channel gating current (Armstrong and Bezanilla, 1974; Neumcke et al., 1976). Its affinity for the channel is not altered by depolarizations that partially or fully inactivate g_{Na} (Ulbricht and Wagner, 1975; Almers and Levinson, 1975; Jaimovich et al., 1976). Local anesthetics also appear to occlude the pore, but unlike TTX they alter gating currents, and their effectiveness is modified by channel activation or inactivation (Khodorov and Belyayev, 1967; Strichartz, 1973; Khodorov et al., 1976; Cahalan, 1978; Yeh and Armstrong, 1978). Inhibition of g_{Na} is promoted by steady or repetitive depolarizations, which are said to produce "voltage-dependent," "use-dependent," or "frequency-dependent" block (Strichartz, 1973; Courtney, 1975; Hille, 1977). These contrasts between actions of TTX and local anesthetics are consistent with evidence that the drugs bind at different sites along the ion path (Strichartz, 1973; Hille, 1978; Cahalan and Almers, 1979), blocking the channel in a noncompetitive manner (Colquhoun et al., 1972; Staiman and Seeman, 1975; Wagner and Ulbricht, 1976).

In heart, analysis of sodium currents has been more difficult, and the distinction between effects of TTX and local anesthetics is not at all clear. For many years now the sodium conductance has been indirectly assessed by measurements of the maximal rate of action potential depolarization, $\dot{V}_{max}$ (Weidmann, 1955*a*; Hoffman and Cranefield, 1960). This approach led to early indications of voltage-dependent and use-dependent effects of local anesthetics in cardiac preparations (Weidmann, 1955*b*; Johnson and McKinnon, 1957; Heistracher, 1971). Because these results have turned out to be consistent with later analysis in nerve and skeletal muscle, they fit the conventional view that sodium channels in the heart are much the same as those in other excitable cells. However, this concept has been challenged by recent experiments of Baer et al. (1976) and Reuter et al. (1978). Using $\dot{V}_{max}$ measurements in ventricular muscle, they reported that in heart, unlike nerve, TTX block of sodium channels is both voltage- and use-dependent.

Possible differences between sodium channels in heart and other excitable tissues are relevant to questions about the basic structure of these channels and the mode of action of antiarrhythmic drugs. However, the conclusions of Reuter and his colleagues remain controversial because of limitations of $\dot{V}_{max}$ as an index of g_{Na}, which could, in principle, produce an artifactual voltage dependence of drug action (Cohen and Strichartz, 1977; Strichartz and Cohen, 1978). Defenders of the $\dot{V}_{max}$ approach (Hondeghem, 1978; Walton and Fozzard, 1979) and critics all agree that voltage-clamp measurements are needed. We have carried out such experiments, using methods recently developed in this laboratory for studying I_{Na} in rabbit Purkinje fibers under good voltage control (Colatsky and Tsien, 1979; Colatsky, 1980). The robustness of these preparations (1–2 h "lifespan") enabled us to examine the kinetics

of TTX block in some detail. We found no steady-state voltage dependence of TTX block. However, we did observe prominent kinetic effects, including use dependence, which has components related to I_{Na} activation and inactivation. Thus, TTX seems to alter channel gating in the heart, but in a significantly different way than the local anesthetics.

Preliminary reports of some aspects of this work have already been published (Cohen et al., 1979; Bean et al., 1980).

METHODS

Sodium currents in rabbit Purkinje fiber preparations were studied using a two-microelectrode voltage clamp, as described previously (Colatsky and Tsien, 1979; Colatsky, 1980). In each preparation used for an experiment, the adequacy of voltage control was confirmed by three criteria: (*a*) rapidly rising and quickly settling voltage traces, (*b*) short capacitative transients (time constants of 0.2–1.3 ms), and (*c*) little or no change in sodium current time-course when current magnitude is changed by inactivation or by application of TTX (see Fig. 1). Some preparations had longer capacitative transients, and these invariably showed changes in sodium current time-course as the current magnitude was changed. The voltage control in these preparations was assumed to be poor, probably because of partial uncoupling of the cells in the preparation, and they were used only for exploratory studies.

To achieve good voltage control, currents were kept small, generally <200 nA, by using solutions of low sodium concentration. To resolve I_{Na} when large concentrations of TTX were applied, it was necessary to increase the sodium concentration in the solution; usually, the increase in sodium concentration was chosen to approximately offset the block by TTX so that the currents were of similar magnitude with and without TTX. In some cases, it appeared that when the sodium concentration was raised, I_{Na} increased more than would be predicted by the independence principle, especially at low (10–40 mM) sodium concentrations. For this reason, experiments in which the absolute level of block by TTX was of interest were always done with no change in the sodium concentration, as in experiments shown in Figs. 1 and 2. Solutions contained concentrations of NaCl and choline-Cl that totalled 150 mM, 4 mM KCl, 1.8 mM $CaCl_2$, 0.5 mM $MgCl_2$, 3.6 mM $MnCl_2$, 5.0 mM dextrose, and 10 mM HEPES, and were titrated to pH 7.4 with ~4.5 mM NaOH. TTX was obtained from Calbiochem-Behring Corp., American Hoechst Corp., San Diego, Calif., and contained ~7 μM citrate/1 μM TTX. 500 μM citrate had no effect on either the magnitude of I_{Na} or the rate of recovery from inactivation.

Peak I_{Na} was measured as (peak inward current) − (steady-state current). Test-pulse potentials were usually chosen to be near the peak of the current-voltage (I-V) relation (−40 to −20 mV with 10–80 mM $[Na]_o$) to minimize the effect of any errors from series resistance or spatial nonuniformity. At these potentials, peak I_{Na} was generally well-separated from the capacitative transient, but linear capacity currents were digitally subtracted when necessary. Calcium current and calcium-activated outward current were inhibited by the Mn in the solution. Leakage current was always very small relative to I_{Na}. Experiments in which large concentrations of TTX were applied to block I_{Na} confirmed the absence of significant steady-state I_{Na}, justifying the subtraction of steady-state current as a correction for leakage current.

Currents were digitized, recorded, and analyzed on a PDP-8 minicomputer (Digital Equipment Corp., Maynard, Mass.). The Patternsearch algorithm (see Colquhoun [1971]) was used to obtain least-squares fits to the dose-response curve and to the inactivation curves.

RESULTS

TTX Block in Steady-State

Voltage-clamp experiments allow a direct analysis of TTX block of sodium channels that can be compared with earlier inferences using maximal upstroke velocity, $\dot{V}_{max}$. Fig. 1 illustrates voltage and current records from a short rabbit Purkinje fiber preparation under a two-microelectrode voltage clamp (Colatsky and Tsien, 1979; Colatsky, 1980). The superimposed traces show net membrane current records evoked by a depolarizing clamp step in the absence of drug and in the presence of 1 μM and 4 μM TTX. Taking the drug-free

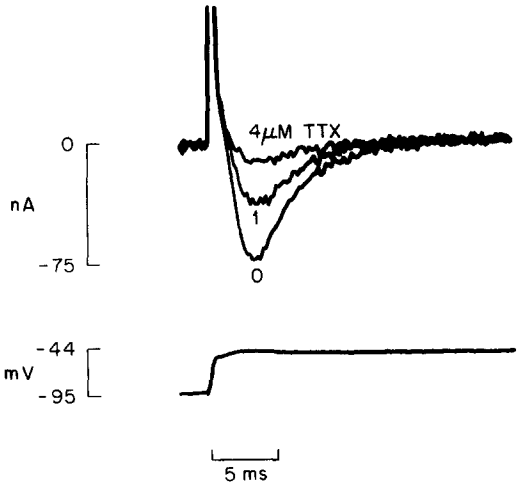

FIGURE 1. Effect of TTX on membrane current. Traces were taken in drug-free solution, and after >5-min exposure to 1 and 4 μM TTX. Before the depolarizing step that evoked I_{Na}, the membrane was held for 45 s at −95 mV where $h_\infty = 0.9$. During a depolarizing step to − 55 mV, the capacity current transient had completely decayed at 3.4 ms, the time-to-peak I_{Na} at −44 mV. Preparation C42-1, 10 mM Na_o, 18°C.

record as 1, the peak sodium current was reduced to 0.55 by 1 μM TTX and to 0.17 by 4 μM TTX. These effects were fully reversible: I_{Na} recovered to 0.98 of control after a 3-min washout in drug-free solution (trace not shown). The records are representative of our other experiments in showing that TTX reduces the amplitude of I_{Na} without significantly affecting its time-course. This holds true even at TTX concentrations as high as 20 μM (see Fig. 13).

The reversibility of the TTX block, and the stability of the rabbit Purkinje fiber preparation, made it possible to study effects over a wide range of drug concentrations during the course of a single experiment. Fig. 2 shows TTX dose-response curves and is concerned with the possible influence of steady membrane potential on TTX binding. The upper set of symbols (●) represents sodium currents evoked from a holding potential (−104 mV) negative enough to completely remove resting inactivation. The symbols are numbered to

indicate the sequence of drug concentrations; the point labeled *5* was taken in the absence of TTX as a check against progressive rundown. The lower set of symbols (■) shows peak I_{Na} during the same series of bathing solutions, as obtained with a less negative holding potential (−89 mV), at which only 0.44 of the channels were available in the absence of drug. Both sets of points are well-fitted by one-to-one binding curves. This is similar to TTX block of sodium channels in other excitable membranes, and it is consistent with the view that a single toxin molecule occludes a single channel (see reviews by

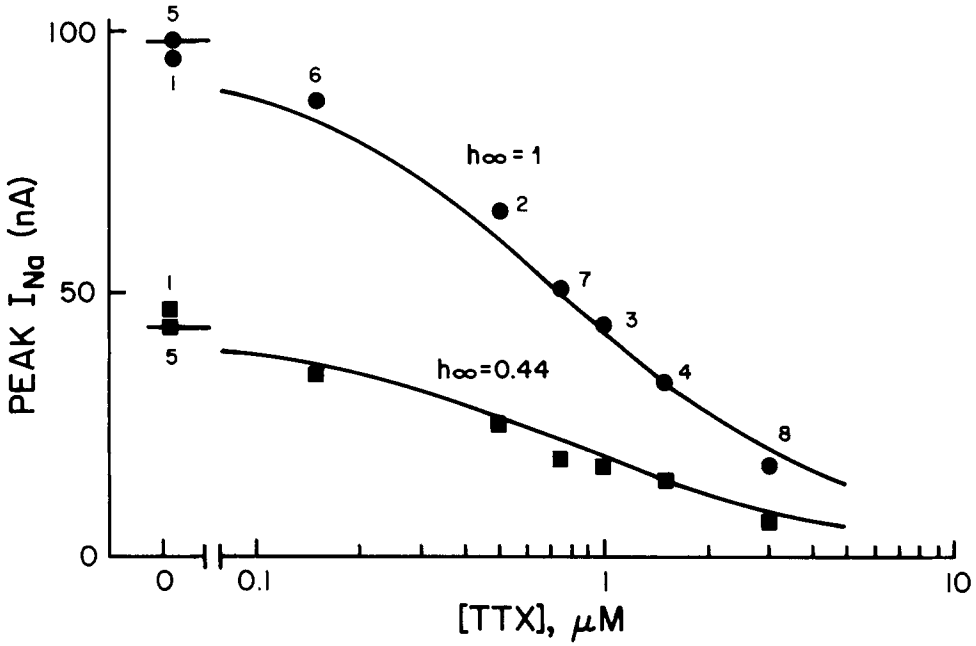

FIGURE 2. Concentration dependence of TTX block at membrane potentials giving different degrees of sodium channel inactivation. I_{Na} was evoked by a test pulse to −44 mV after 45 s at −104 mV (●) or −89 mV (■). Numbers indicate sequence of solutions. Upper curve is a least-squares fit using the expression $I_{Na} = \hat{I}_{Na}/(1 + [TTX]/K_D)$, where $\hat{I}_{Na}$ = 98.7 nA, K_D = 0.82 μM. Lower curve is the same expression, scaled by 0.44 to allow for I_{Na} inactivation. Preparation C44-1, 10 mM Na_o, 18°C.

Hille [1970]; Narahashi [1974]; Ulbricht [1977]; Ritchie and Rogart [1977]). The point of half-inhibition corresponds to the dissociation constant, K_D, of the toxin-receptor complex. A value of 0.82 μM was used in the least-squares fit to the data in this experiment; the results in Fig. 1 correspond to a K_D of 1.16 μM. These results are typical of a total of 12 preparations where single or multiple toxin concentrations were studied at constant external sodium (values for K_D averaged 0.76 μM). Our estimates of TTX binding from voltage-clamp measurements of I_{Na} are in qualitative agreement with earlier results using $\dot{V}_{max}$, which suggested that, in comparison with sodium channels of most

nerve and skeletal muscle membranes, sodium channels of mammalian heart are several orders of magnitude less sensitive to TTX (Dudel et al., 1967; Sano et al., 1968; Yanaga and Holland, 1970; Carmeliet and Vereecke, 1969; Scholz, 1969; Baer et al., 1976; Coraboeuf et al., 1979).

Perhaps the most interesting aspect of Fig. 2 is the issue of possible interaction between TTX block and sodium channel inactivation. This was prompted by the work of Baer et al. (1976), who measured $\dot{V}_{max}$ in guinea pig ventricular muscle. They found that an 18-mV depolarization, which reduced $\dot{V}_{max}$ by 35% in the absence of TTX, lowered the concentration needed for half-maximal inhibition from 14 to 1.2 μM. By way of contrast, both sets of symbols in Fig. 2 are well-fit by smooth curves drawn for the same value of K_D. In our voltage-clamp experiments, the binding of TTX seems to be more or less unaffected by steady membrane potential or maintained sodium inactivation. Put in a different way, the degree of inactivation at −89 mV—given by the percentage reduction between upper and lower symbols—seems to be the same regardless of the TTX concentration.

This conclusion was supported by experiments studying steady-state inactivation over a range of potentials in the absence and presence of TTX. In these experiments, resolution of I_{Na} was maintained by offsetting the effects of toxin with a compensatory increase in Na_o (see Methods). Fig. 3 shows results from runs in 0 mM TTX, 10 mM Na_o, and 2 μM TTX, 20 mM Na_o. After the membrane had been held for >15 s at various potentials between −110 and −70 mV (abscissa), I_{Na} was evoked by a step to a test potential at the peak of the I–V curve in each solution. In the absence of toxin (○), the sodium current magnitude (*ordinate*) shows the usual sigmoid dependence on prepotential level (*abscissa*). This relationship seems to be unaffected by TTX: least-squares fits (*smooth curves*) give practically identical values for the midpoint voltage V_h with and without toxin (*arrows*). The voltage parameter κ, which determines the steepness of the sigmoid curve, was also virtually unchanged.

By using increases in Na_o to compensate for TTX block, we were able to determine I_{Na} availability curves in the presence of very high toxin concentrations. As Table I indicates, very little change in V_h was observed even with 20 μM TTX; the average change in V_h in three experiments of this type was only −2.3 mV. It made little difference whether the effect of the toxin on the absolute size of I_{Na} was left uncompensated (Fig. 2) or overcompensated with Na_o, as in Fig. 3.

These results are consistent in failing to show significant interaction between TTX block and sodium inactivation under steady-state conditions. A slight interaction cannot be excluded, but there was no sign of a prominent decrease in K_D with depolarization (Baer et al., 1976) or a pronounced hyperpolarizing shift in V_h with toxin (Reuter et al., 1978). A similar conclusion was reached in a study of TTX-sensitive background currents in dog Purkinje fibers by Colatsky and Gadsby (1980). In their voltage-clamp experiments, the response to toxin was fitted by one-to-one binding curves with $K_D \cong 1.2$ μM TTX; the sensitivity to TTX was, if anything, slightly *decreased* by depolarization.

The discrepancy between our results and those of Baer et al. (1976) is

interesting because it would be expected if $\dot{V}_{max}$ were a nonlinear index of cardiac sodium conductance (see Introduction). Direct comparisons between measurements of $\dot{V}_{max}$ and I_{Na} are obviously desirable. Under the experimental conditions of Baer et al.—guinea pig papillary muscle near 37°C—reliable voltage-clamp recordings of I_{Na} are not yet possible. On the other hand, action

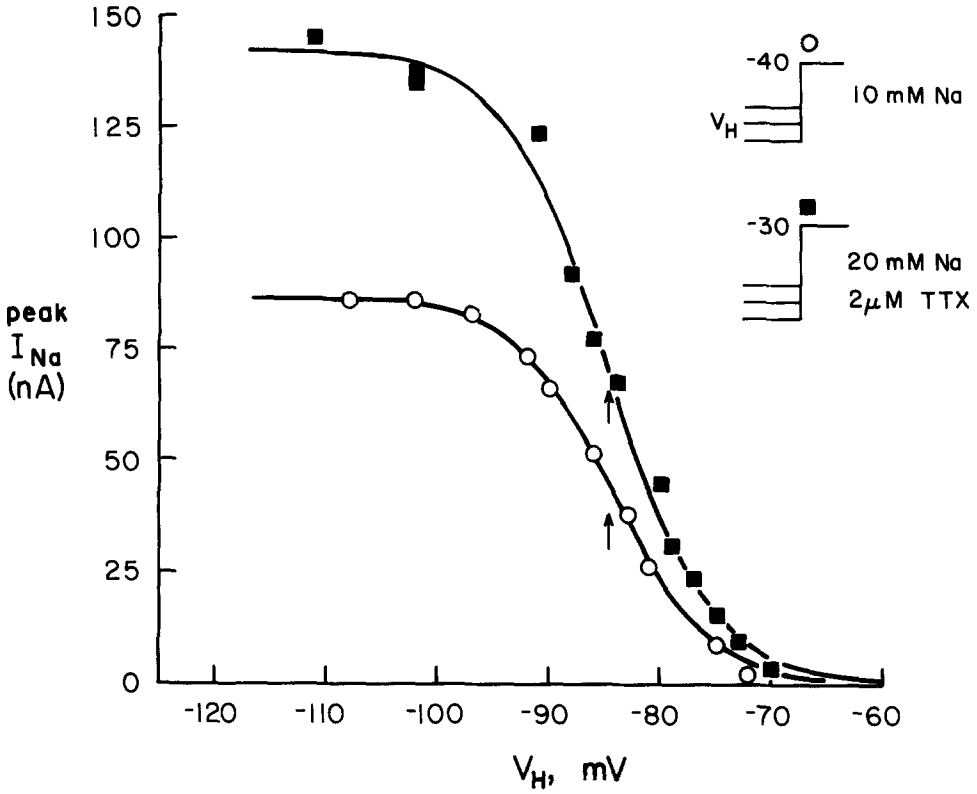

FIGURE 3. Voltage-dependence of I_{Na} availability with and without 2 μM TTX. I_{Na} availability was measured with a constant test pulse after a 15–18-s period during which the holding potential, V_H, was set to the value indicated. The test pulse was chosen to be at the peak of the *I-V* relation in each case, at −40 mV in the absence of drug (Na_o = 10 mM) and at −30 mV in TTX (Na_o = 20 mM). Note that the changes in Na_o and test potential overcompensate for the block by TTX. Smooth curves are least-squares fits to the data using the expression and parameters given in Table I. *Arrows* indicate the midpoints of the theoretical curves. Preparation C33-1, 18°C.

potential upstrokes can be recorded in rabbit Purkinje fibers over a wide range of temperature, so it is relatively straightforward to ask whether $\dot{V}_{max}$ is proportional to available g_{Na} in our preparations. Taking this approach, we have found that $\dot{V}_{max}$ is much less sensitive than I_{Na} to block by TTX (C. J. Cohen et al., 1981), or to inactivation by steady depolarization (C. J. Cohen, B. P. Bean, and R. W. Tsien, unpublished data). Thus, $\dot{V}_{max}$ is a nonlinear

measure of available sodium conductance in rabbit Purkinje fibers, much the same as in nerve (Ulbricht and Wagner, 1975) or skeletal muscle (Colquhoun et al., 1974; Pappone, 1980), as might be expected from theoretical arguments (Hunter et al., 1975; Khodorov and Timin, 1975; Cohen and Strichartz, 1977; Strichartz and Cohen, 1978; I. S. Cohen et al., 1981). Questions about the relationship between $\dot{V}_{max}$ and available sodium conductance in other cardiac preparations must await suitable voltage-clamp experiments.

Use-dependent Block

Use-dependent or frequency-dependent block is another aspect of TTX action that was first suggested by $\dot{V}_{max}$ measurements (Robinson and Sleator, 1977; Reuter et al., 1978; Mary-Rabine et al., 1979). In this case, we were able to

TABLE I

VOLTAGE DEPENDENCE OF I_{Na} AVAILABILITY WITH AND WITHOUT TTX

Experiment	[TTX]	$[Na]_o$	I_{max}	κ	V_h	ΔV_h
	(μM)	(mM)	(nA)	(mV)	(mV)	(mV)
C33-1	0	10	86.6	4.32	−84.4	−0.2
	2	20	142.5	4.59	−84.6	
C49-1	0	10	53.9	4.78	−82.0	−5.1
	20	60	122.6	4.81	−87.1	
C50-2	0	10	58.0	4.79	−84.8	−1.7
	20	40	44.9	5.62	−86.5	

The dependence of test-pulse I_{Na} on holding potential was fit by $I_{max}/(1 + \exp[V_H - V_h]/\kappa)$ using a least-squares method which allowed I_{max}, V_h, and κ to all vary. Holding potentials were established long enough (>2 s without TTX; >15 s with TTX) to reach a steady state.

confirm the earlier results under voltage-clamp conditions. Fig. 4 illustrates how TTX block can be dramatically enhanced by repeated depolarizations. Trains of 50-ms pulses to −40 mV were applied at 2.5 Hz after a long rest period. In the absence of drug, I_{Na} changes very little from pulse to pulse (Fig. 4*C*). The 1st and 10th sodium currents are almost exactly superimposable (Fig. 4*A*), as expected if repriming of sodium channels reaches completion during the 350-ms intervals between successive pulses (see Colatsky [1980]; and below). In the presence of 2 μM TTX (with Na_o raised to maintain I_{Na}), the same pattern of depolarizations results in a prominent decline in the amplitude of I_{Na} from one pulse to the next (Fig. 4*B* and *C*). After 10–15 pulses, the decline levels off with I_{Na} at 0.55 of its amplitude during the first pulse after the long rest period. Similar effects of repetitive depolarizations were observed in other experiments.

Use-dependent block of sodium channels in the heart is not new. It has been known for some time that local anesthetics such as quinidine or lidocaine show such behavior (see, for example, Johnson and McKinnon [1957]; Heis-

tracher [1971]; Chen et al. [1975]), but the use dependence is generally thought to be accompanied by substantial shifts in the voltage dependence of channel availability (see Weidmann [1955*b*]; Hondeghem and Katzung [1977]; Hille, [1978]). Previous studies have relied on $\dot{V}_{max}$, but recent voltage-clamp experiments also show shifts with quinidine or lidocaine (Brown et al., 1980; Bean et al., 1981). The action of TTX on rabbit Purkinje fibers is particularly intriguing because use-dependent effects (Fig. 4) appear divorced from steady-state effects (Figs. 2 and 3). As a phenomenon, TTX block of

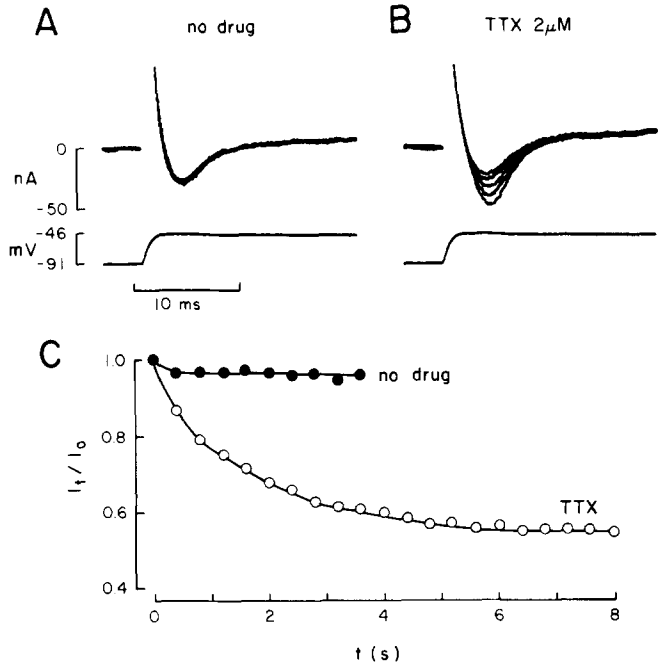

FIGURE 4. Use-dependent effect of TTX. Membrane currents during trains of 50-ms pulses from −91 to −46 mV at 2.5 Hz after a rest period of 11 s. (A) Records taken with no TTX, 20 mM Na_o, during pulses 1 and 10 of the train. (B) Records in 2 μM TTX, 35 mM Na_o, during pulses 1, 2, 4, 8, and 16. (C) sodium current amplitudes from the same runs, plotted as a fraction of the first I_{Na} of each train. Preparation T92-1, 18°C.

these cardiac sodium channels seems to be an intermediate case between TTX block in nerve (neither use dependence nor steady voltage dependence) and local anesthetic block in both nerve and heart (both use dependence and steady voltage dependence).

Extra Block as an Aftereffect of Depolarization

The rest of this paper is aimed at understanding the kinetic basis of the use-dependent TTX block. In earlier studies of use-dependent block produced by local anesthetics, most investigators relied on the application of long trains of

pulses—often as a means of accentuating the relatively small aftereffects left by individual pulses. This approach is not necessary in the present case because the aftereffect of even a single pulse can be quite large. For quantitative analysis, we found it more convenient to use a simple two-pulse procedure (Hodgkin and Huxley, 1952; Khodorov et al., 1976). The idea was to see how the first depolarization ("conditioning pulse;" level, V_c; duration, t_c) influenced the sodium current evoked by a second depolarization ("test pulse;" level, V_t). The conditioning and test pulses are separated by a variable interval (level, V_p; duration, t_p). To emphasize relative changes in the size of I_{Na}, results will often be presented as the ratio $I_{Na}(test)/I_{Na}$ (conditioning), abbreviated I_t/I_c. Care was taken to leave an ample quiescent period before each pulse pair to allow aftereffects of earlier pulse pairs to subside completely.

Fig. 5 shows how TTX influences the recovery of sodium current after a 5-s conditioning pulse. In each run, I_{Na} is normalized to its value after a long rest interval to emphasize relative recovery instead of tonic block. In the absence of toxin (Fig. 5*A*, ○), the test sodium current recovers more or less exponentially as the interval between pulses is prolonged. The time constant of repriming, τ_r = 140 ms, fits with earlier analysis of recovery from sodium inactivation after brief pulses (Colatsky, 1980). Even after the 5-s pulse used here, there is no indication of slow recovery from inactivation like that found in nerve (see Meves [1978] for a review) or skeletal muscle (Schwarz et al., 1977; Harvey et al., 1979). TTX affects the recovery in a dose-dependent manner. In 1 μM TTX, ~60% of the sodium current reprimes with the same exponential time-course as in the absence of the drug, but recovery of the remaining 40% barely begins within a period of 1 s. When the TTX concentration is increased to 10 μM (with a simultaneous increase in Na_o to preserve resolution of I_{Na}), the slowly recovering component grows to ~80%. Fig. 5*B* plots the data in Fig. 5*A* and additional points from the same experiment to show the complete time-course of recovery. In both 1 and 10 μM TTX, the slow-recovery phase shows an exponential time-course with a time constant of 4–5 s. Because this time constant is more than an order of magnitude greater than τ_r, there is no difficulty in dividing the sodium channels into two groups: channels undergoing normal recovery from inactivation, and channels showing slow recovery from the extra block resulting from the conditioning depolarization. It is the accumulation of this extra block that gives rise to use dependence during repeated depolarizations.

The extent of extra block is not only dependent on the toxin concentration, but also on the duration of the conditioning pulse. Fig. 6 shows results from another experiment in which the dose of TTX was kept at 10 μM. A 5-s conditioning pulse (△) leaves behind a large amount of extra block; the magnitude and time-course of this slow component are in good agreement with the results in Fig. 5*B*. Prolonging the conditioning pulse from 5 to 15 s produces no change in the amount of extra block or its time-course of decay. Abbreviating the conditioning pulse to 0.3 s reduces the degree of extra block, but once again, the time-course of recovery remains unchanged. In another experiment, nearly equal recovery time constants were obtained after conditioning pulses lasting 50 ms and 5 s.

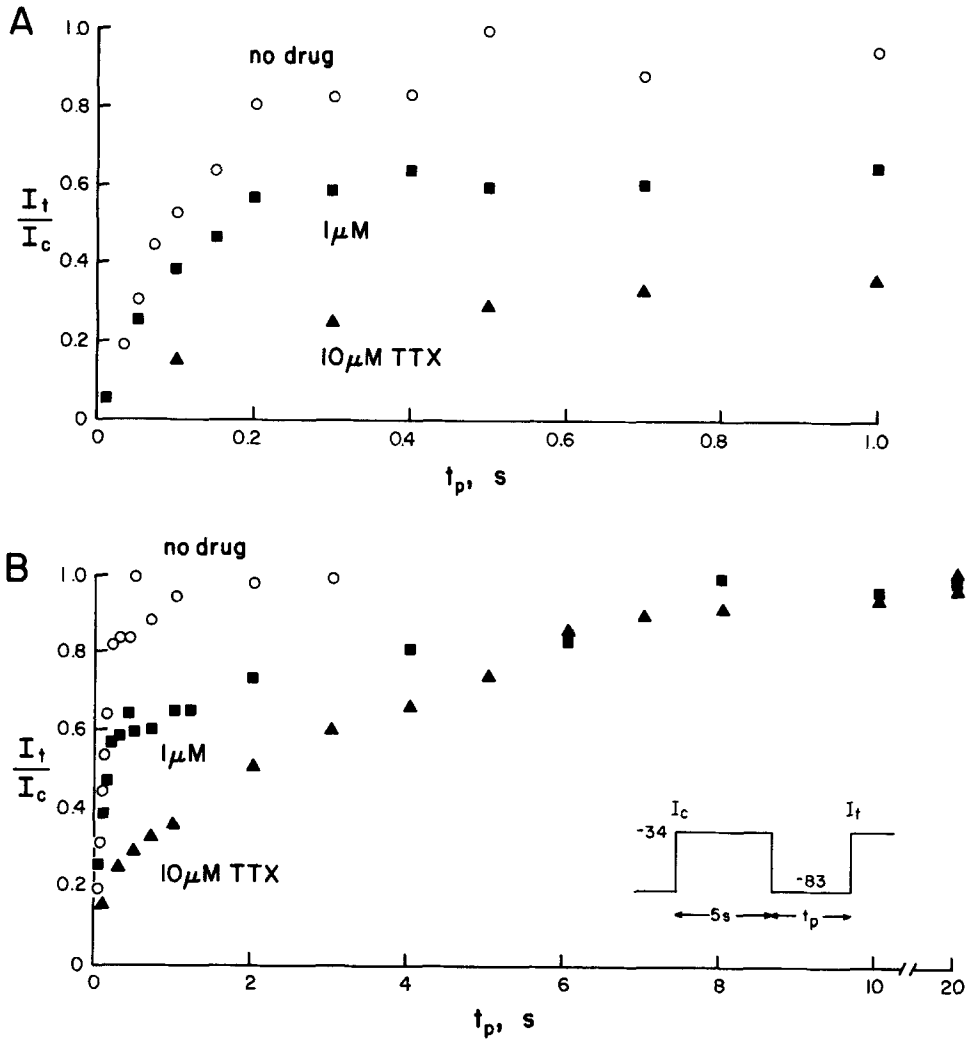

FIGURE 5. Effect of TTX on I_{Na} repriming as studied by a two-pulse procedure. Results plotted on expanded (*A*) and slow (*B*) time bases. Sodium currents were evoked by a test pulse at a varying interval (t_p) after a 5-s conditioning pulse. Sodium current during the test depolarization (I_t) was normalized by I_{Na} during the immediately preceding conditioning pulse (I_c). Records taken during consecutive runs at 0 TTX, 10 mM Na_o (○); 1 μM TTX, 10 mM Na_o (■); and 10 μM TTX, 80 mM Na_o (▲). Preparation C43-1, 18°C.

Voltage Dependence of Extra Block

Figs. 5 and 6 describe how extra block develops as a function of toxin concentration and time, respectively. In both instances, we found a wide disparity between the time constants for recovery from normal inactivation and removal of extra block. An interpulse interval of 0.5 or 1 s allowed

removal of normal inactivation to approach steady-state, but produced relatively little recovery from extra block. In Fig. 7 we use this approach to characterize the voltage-dependent development of extra block. 5-s conditioning pulses to various potential levels were imposed from a holding potential of −97 mV. The aftereffects of these pulses were assessed after a 0.5-s interval by measuring I_{Na} (▲) during a test depolarization to −35 mV. The results show that substantial persistent block can be produced by long-lasting depolarizations to levels that do not elicit significant I_{Na} (<−50 mV in this experiment). The voltage-dependence seen with 5-s pulses is rather similar to the voltage-dependence of steady-state channel availability in the presence of TTX, as determined in the same experiment (*circles*). With respect to voltage depen-

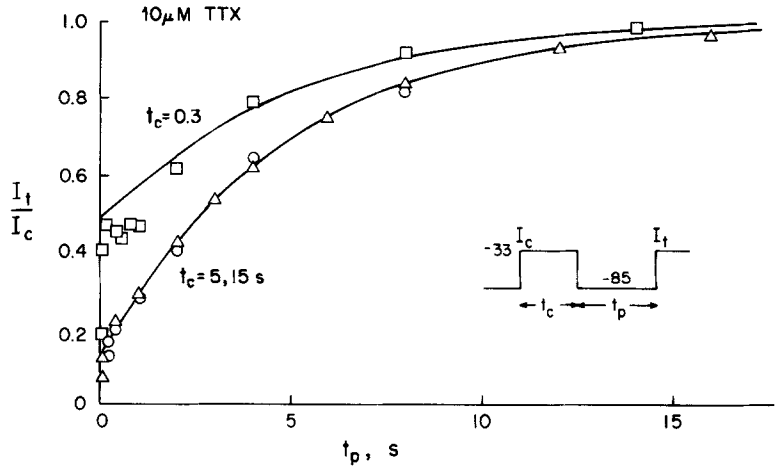

FIGURE 6. Slow recovery of I_{Na} in 10 μM TTX after conditioning pulses lasting 0.3 s (□), 5 s (△), or 15 s (○). Smooth curves are exponentials fitted by eye. τ = 4.95 s. Preparation C4-7, 155 mM Na_o, 16°C.

dence, the extra block with TTX resembles the extra block seen with procaine or trimecaine in frog node by Khodorov et al. (1976), who refer to the phenomenon as "slow sodium inactivation."

Reconciling Steady-State and Time-dependent Aspects of TTX Block

It is important to distinguish between steady-state and kinetic effects in interpreting the results up to this point. Under the steady-state conditions studied in Figs. 2 and 3, tonic TTX block seems to be virtually independent of voltage. However, under conditions that are definitely not steady-state, as in Fig. 7, there appears an extra component of block that shows a marked voltage dependence. Because this combination of phenomena is novel for a channel-blocking molecule, it may be helpful to present a simple kinetic interpretation which shows how the various findings can be reconciled. In this scheme (Fig. 8, *top*), channels undergo transitions between resting (R) and inactivated (I) states. Opening of channels, although not explicitly considered,

can be used to assess those channels available in the R state. The rate constants between R and I are the conventional Hodgkin-Huxley parameters α_h and β_h, that determine h_∞ [$h_\infty = \alpha_h/(\alpha_h + \beta_h)$], the fractional availability of channels in the absence of toxin. Both R and I can take on toxin (T) with the same equilibrium dissociation constant, K_D (where $T/K_D = k/\ell$). However, there is an ω-fold ratio between the rates at which the binding reactions approach equilibrium. k and ℓ are assumed to be independent of voltage. The toxin-blocked states RT and IT are connected by rate constants similar in voltage dependence to α_h and β_h, but scaled ν-fold.

Set up in this way, the scheme conforms to the observation that toxin-

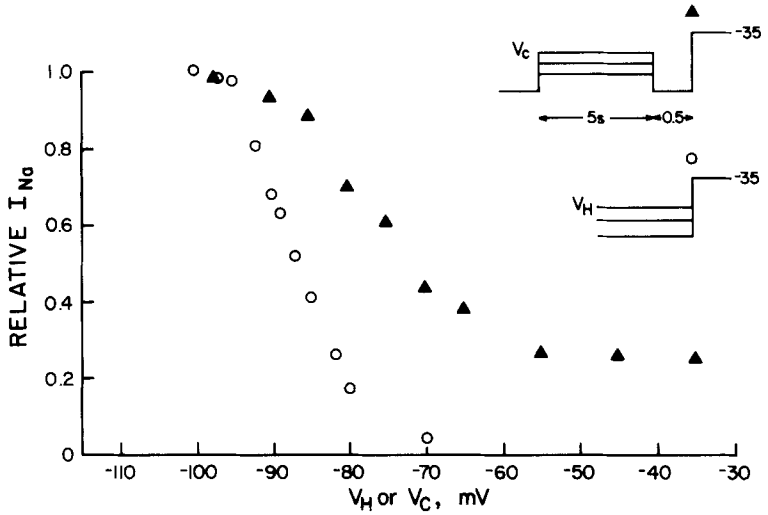

FIGURE 7. The voltage dependence of extra block compared with the voltage dependence of channel availability. ▲, peak test currents after 5-s conditioning pulses to V_c and a 0.5-s return to −97 mV. O, availability curve, with holding potentials established for at least 15 s before the test pulse. All currents are normalized with respect to peak test current with $V_H = -97$ mV. Both protocols performed with 10 μM TTX, 20 mM Na_o. Preparation C55-3, 17°C.

binding and steady-state inactivation appear independent, and also satisfies the presumption of microscopic reversibility. It is similar (and different) from the modulated receptor hypothesis for local anesthetics (Hille, 1977; Hondeghem and Katzung, 1977) in that the state of the channel affects the speed of toxin binding (but not the affinity), and that block by toxin influences speed of inactivation and repriming (but not the degree of inactivation and repriming).

Kinetic aspects of TTX block can be qualitatively explained within this framework. The existence of a slowly repriming fraction indicates that TTX-blocked channels reprime much more slowly than unblocked channels (that is, $\nu \ll 1$). The role of extra block can be assigned to the state IT: this takes into account observations that the extra block is increased by raising toxin concentration or by depolarizations that inactivate the channels.

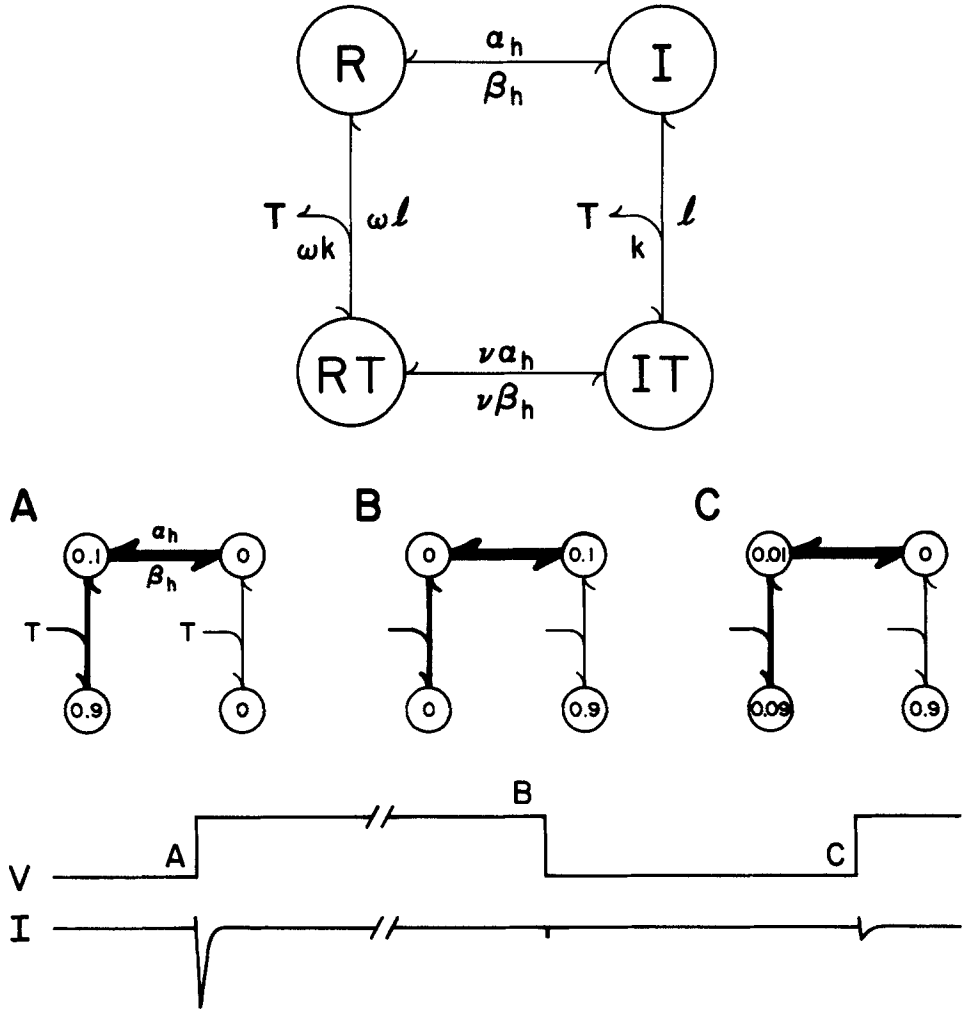

FIGURE 8. A simple scheme for reconciling steady-state and kinetic aspects of TTX block. Extra block is accounted for as a long-lasting perturbation away from the equilibrium distribution among channel states. In the upper panel, k and ℓ are forward and backward rate coefficients in units of s^{-1}, and ω and ν are dimensionless coefficients which determine the relative speed of reactions. The model assumes that toxin binding and inactivation are independent at equilibrium because no such interaction could be detected experimentally (cf. Reuter et al. [1978], p. 138 and Hille [1978], Fig. 11). In the lower panels, the fractional occupancy is indicated at the beginning and end of a long depolarization (A and B, respectively), and at the end of a brief repolarization (C). The relative speed of reactions is indicated schematically by the thickness of the arrows. The corresponding two-pulse voltage-clamp protocol and the relative I_{Na} elicited by these pulses are schematically indicated at the bottom. The time at which panels A, B, or C occur is indicated on the *voltage trace*. For further details, see text.

The *lower panels* of Fig. 8 give a specific example of how extra block could occur during a two-pulse experment. For numerical simplicity, we treat a limiting case where $\nu = 0$, $\omega \gg 1$, and $T/K_D = 9$. Fig. 8*A* shows the equilibrium distribution of channels at a potential where inactivation is completely removed: 0.1 of the channels are in R and 0.9 are in RT. Fig. 8*B* shows the expected distribution after a long depolarization to a potential where inactivation is complete: channels reach equilibrium with 0.1 in I and 0.9 in IT. There is no net binding or unbinding of toxin by the end of the depolarization, because 0.9 of the channels are toxin bound at A or B, but channels originally in state RT must sequentially unbind and then rebind toxin to reach IT. Fig. 8*C* illustrates the effect of following the depolarization with a 1-s repolarization. This is long enough for toxin-free channels to completely recover from inactivation and, with $\omega \gg 1$, it is long enough for the R to RT transition to nearly reach equilibrium while allowing only negligible conversion of IT to I. Thus, to a first approximation, channels that are in I at the beginning of the repolarization distribute to equilibrium between R and RT, whereas channels in IT do not reprime at all. This approximation therefore predicts that at the end of the 1-s repolarization, there will be 0.01 channels in R, 0.09 in RT, and 0.9 in IT. The extra block induced by the conditioning pulse has reduced the test pulse current to 10% of the conditioning pulse current, which already was only 10% of the current with no toxin present.

The kinetic scheme shown in Fig. 8 is intended to serve only as a framework for understanding the basic results of the experiments showing extra block. Although it is too simple to account for all aspects of the results (see Discussion), the scheme makes several testable predictions about the kinetics of development and removal of extra block. First, the model predicts that the rate of recovery from extra block will be rather insensitive to toxin concentration, because the slowest step in the recovery pathway is IT → I, and this will not change with toxin concentration. Second, the model likewise predicts that the rate of recovery will not depend strongly on the membrane potential, because IT → I is postulated to be voltage independent. Third, the rate of development of extra block will be strongly dependent on the free toxin concentration, because the rate-limiting step is postulated to be the binding of toxin to I to form IT.

We performed experiments designed to test each of these predictions. Evidence has already been presented showing that the rate of recovery from extra block is more or less independent of toxin concentration: the experiment in Fig. 5 was performed specifically to test this prediction and, as already noted, the time-course of recovery from extra block was very similar in 1 and 10 μM TTX.

Recovery at Different Membrane Potentials

Fig. 9 shows the results of an experiment that tested whether the rate of recovery from extra block is dependent on membrane potential. With 10 μM 0TTX, a saturating degree of extra block was produced with a 5-s conditioning

pulse and the time-course of recovery was followed by varying the interval between pulses, as in Figs. 5 and 6. The procedure was repeated using three different membrane potentials during the interpulse interval: −84, −94, and −104 mV. Over this 20-mV range, the rate of recovery from inactivation in the absence of TTX usually increased more than fivefold. In contrast, the time-course of recovery from extra block does not show a similar pattern of voltage dependence over these potentials. This result is consistent with the idea that dissociation of toxin could be the slowest step in the recovery from extra block.

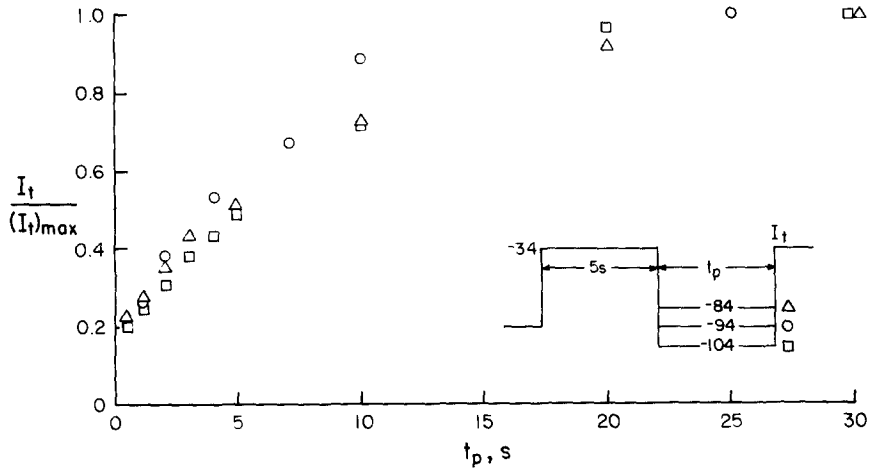

FIGURE 9. Recovery from extra block at three membrane potentials over the range where steady-state inactivation is steeply voltage dependent. Relative peak test pulse current is plotted as a function of the recovery interval. Test pulse currents are normalized with respect to the largest currents obtained at each recovery potential (t_p = 30 s for V_p = −84 and −104 mV; t_p = 25 s for V_p = −94 mV). Preparation C34-3, 10 μM TTX, 80 mM Na_o, 17°C.

Toxin Dependence of the Rate of Onset of the Extra Block

Fig. 10 shows the results of an experiment intended to test whether the development of extra block is faster in higher toxin concentrations. The development of extra block in 1 and 10 μM TTX was followed by varying the conditioning pulse duration in a standard two-pulse protocol. Fig. 10 shows that the development of extra block is faster and more complete in 10 μM TTX, as predicted by the kinetic scheme in Fig. 8. However, the most striking feature of Fig. 10 is the unexpected presence of two distinct phases in the development of extra block: a very fast phase, which produces a significant amount of extra block in 10 ms (the earliest points in Fig. 10), and a much slower phase, which is well-described by an exponential decay to an asymptote. The extra block develops more quickly as the TTX concentration is increased

because the effect at 10 ms is larger and the subsequent exponential onset is faster. The time constant of the exponential phase is 3.2 s in 1 μM and 0.81 s in 10 μM TTX. This change in time constant, and the change seen in two other similar experiments, is quantitatively consistent with the idea that the rate-limiting step in the slow phase is the binding of free toxin to the channel, as in the kinetic scheme in Fig. 8. However, it should be noted that the asymptotic values of extra block achieved in 1 and 10 μM TTX do not differ by as much as would be predicted by the simple scheme in Fig. 8. High doses of TTX do not produce as much extra block as predicted by that model. The change in $[Na]_o$ cannot account for this result, because TTX block has little

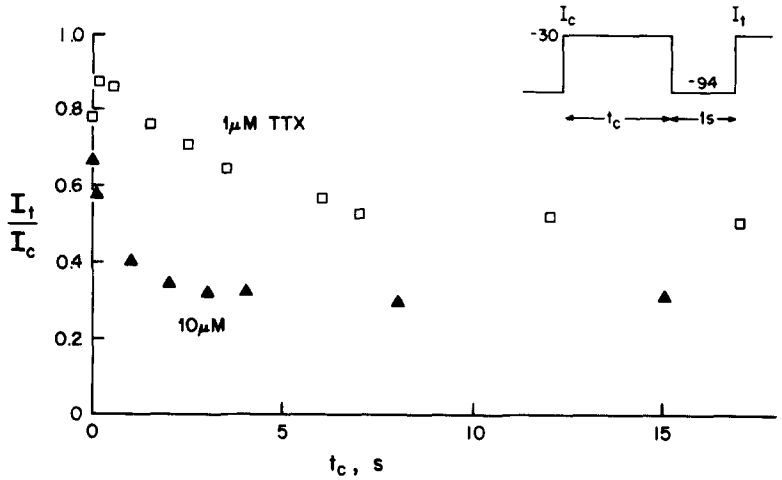

FIGURE 10. Fast and slow components in the development of extra block in 1 and 10 μM TTX. Peak test pulse currents (I_t) are normalized with respect to the peak conditioning pulse current (I_c) and plotted as a function of the conditioning pulse duration. An increase of $[Na]_o$ from 20 to 60 mM accompanied the increase in TTX concentration. Preparation C47-1, 19°C.

or no dependence on $[Na]_o$ (Bean et al., 1981*a*). Similar discrepancies were seen in two other experiments in which the amount of extra block produced by high and low doses of TTX was compared. This point is considered in the Discussion, where more complete kinetic models are considered. A second feature of Fig. 10 that does not fit with the simple scheme is the existence of the fast phase. It will be shown in the following sections that this phase appears to be linked with the activation of channels during the conditioning pulse, which is not explicitly included in the scheme in Fig. 8.

Time-Course and Voltage Dependence of the Fast Phase

Fig. 11 shows the time-course of development of the extra block in 10 μM TTX as in Fig. 10, but in a different fiber and with focus now on the first 50 ms. On this expanded time scale, the slow phase of extra block is barely

evident, but the development of the fast phase can be seen to extend over the first 10 ms of the conditioning pulse. The main purpose of this experiment is to show the similarity between the onset of the fast phase (○) and channel activation during the conditioning pulse (△). The conditioning pulse was deliberately set at a rather negative potential (−38 mV) to slow I_{Na}. Channel activation— or, more strictly speaking, channel openness—was assessed by taking the integral of the sodium permeability during the conditioning pulse, normalizing it, and plotting it on a downward scale (*right ordinate*). The integral measures the degree to which channels have dwelt in the open state during the conditioning procedure. The results show that the fast phase has

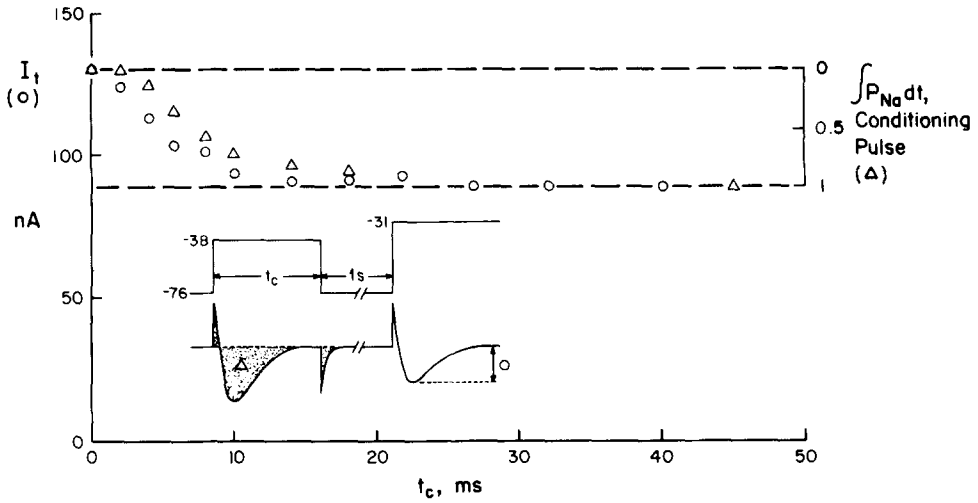

FIGURE 11. Development of extra block with short conditioning pulses. Test currents, I_t (left ordinate, ○), are compared with the time intergrals of sodium permeability associated with conditioning pulses, (right ordinate, △). The baseline for integration was the steady holding current at −76 mV; the integrations included the on and off current transients to give cancellation of on and off capacitative currents and to include tail currents in the integration. No allowance was made for the different driving force during the tail currents, which were very brief. Preparation C37-1. 10 μM TTX, 80 mM Na_o, 19°C.

a sigmoid onset, rather similar to that of channel openness. The fast phase and the build-up of the integral both reach completion at ~10–15 ms. At intermediate conditioning pulse durations (5 ms), extra block slightly precedes channel openness. The overall similarity suggests that the rate at which channels become slowly repriming might be related to the fraction of sodium channels that are activated. The next experiment tested whether the voltage dependence of the fast phase was consistent with such a link.

In Fig. 12, the voltage dependence of channel opening during a 20-ms conditioning pulse and the amount of extra block that is produced by the pulse are compared. The occupancy of the open state was measured by taking the time integral of P_{Na}. Activation of channels and the fast phase of extra

block both depend very steeply on membrane potential in the range from −50 to −30 mV. The two are not correlated perfectly; the voltage dependence of persistent block is ~5 mV negative to the voltage dependence of the time-integral of P_{Na}. However, the overall similarity of the curves reinforces the conclusion that the fast phase is linked in some way with the activation of channels.

DISCUSSION

These experiments show that TTX block of cardiac sodium channels is significantly different than expected from previous measurements of $\dot{V}_{max}$ in

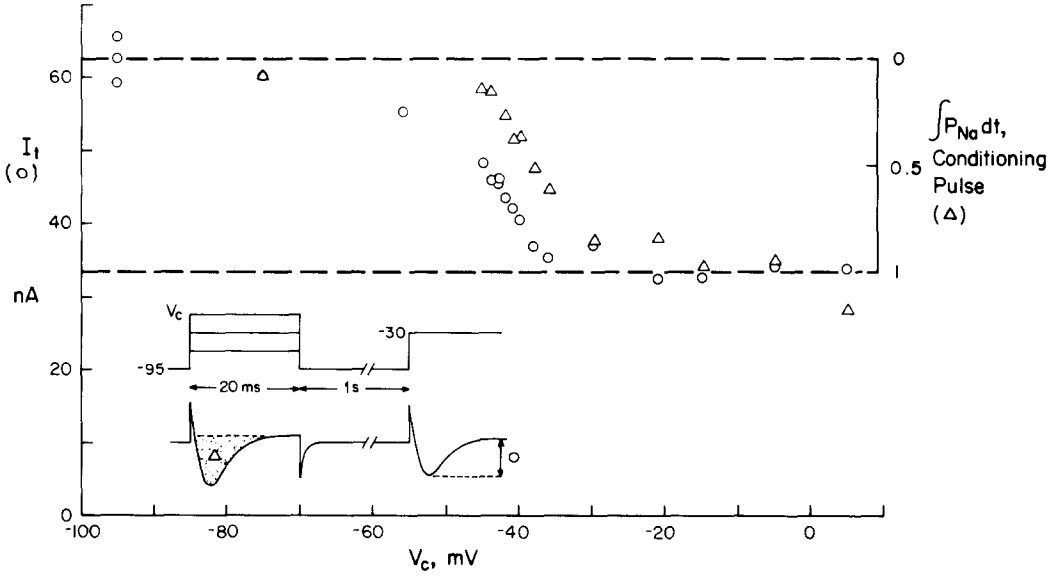

FIGURE 12. Voltage dependence of sodium current activation and the fast phase of extra block. The baseline for integrating the conditioning pulse sodium current was the value of current at the end of the depolarization, by which time inactivation was complete. The Goldman-Hodgkin-Katz equation was used to convert currents to permeabilities (see Colatsky [1980]). Preparation C34-3, 10 μM TTX, 80 mM Na_o, 17°C.

heart or I_{Na} in nerve or skeletal muscle. In contrast to inferences from $\dot{V}_{max}$ (Baer et al., 1976), our voltage-clamp experiments suggest that TTX and steady depolarization act independently in reducing the number of available sodium channels. Unlike nerve (e.g., Courtney [1974]; Gage et al. [1976]), rabbit Purkinje fibers respond to TTX with striking changes in sodium channel kinetics: depolarizing pulses leave aftereffects on channel availability lasting ~100 times longer than normal inactivation (see also Robinson and Sleator [1977]; Reuter et al. [1978]; Mary-Rabine et al. [1979]).

The lack of voltage dependence of steady-state block (Figs. 2 and 3) implies that resting and inactivated channels bind toxin with virtually the same

affinity and that the steady-state voltage dependence of inactivation is unchanged by the binding of toxin. On the other hand, the slow component of repriming in the presence of toxin (Figs. 5, 6, and 9) indicates that toxin-blocked channels move between resting and inactivated states at much slower rates than toxin-free channels. Thus, although channel gating need not alter the affinity of the channel for TTX, TTX binding influences the kinetics of channel gating. In this respect, sodium channels in mammalian heart may be fundamentally different from those in nerve, where toxin block and channel gating seem independent.

It is interesting to compare TTX with local anesthetics such as quinidine or lidocaine, which are often used clinically as antiarrhythmic drugs. Even though TTX and tertiary amine anesthetics have very different structures and presumably act at separate sites within the channel, they can produce similar effects on the history dependence of I_{Na}. This is seen rather clearly during repetitive depolarizations that elicit significant I_{Na} as "frequency-dependent" or "use-dependent" block. We relied on the more general term "extra block" in most of this paper because it encompasses prolonged aftereffects produced by a single, weak depolarization that fails to activate significant I_{Na}, as well as multiple depolarizations that clearly open channels. Indeed, one of the main conclusions of the paper, obtained by varying the level and duration of conditioning pulses, is that extra block can develop in two ways: rapidly, in association with channel activation, or slowly, in association with channel inactivation. There are reasons for thinking that, whichever way it is produced, extra block seems to reflect the same slowly decaying state(s) of the channel. First, the decay of extra block has the same time constant after a brief depolarization or a long-lasting one (p. 392). Second, a saturating degree of extra block can be produced by a long pulse to −60 mV; although stronger depolarizations evoke clear surges of sodium current, and extra block related to activation, the final degree of block is no greater (Fig. 7).

Is Rapidly Developing Extra Block a Result of TTX Binding to Open Channels?

Fast drug binding to open sodium channels must be considered as a possible explanation for rapidly developing extra block. This kind of mechanism has received considerable experimental support in the cases of local anesthetic block of excitable sodium channels (Strichartz, 1973; Courtney, 1975; Hille, 1977) as well as acetylcholine-activated channels (Adams, 1976; Ruff, 1977; Neher and Steinbach, 1978). If applicable to TTX and sodium channels in heart, it could explain why rapidly developing extra block and channel activation are closely correlated in their time and voltage dependence.

Some of the difficulties with this type of explanation are illustrated in Fig. 13, using a basic kinetic framework proposed by Hille (1977) and Hondeghem and Katzung (1977) for local anesthetics. The model (Fig. 13*A*) adds two activated states, A (conducting) and AT (blocked), to the resting and inactivated states of Fig. 8. In our considerations, rate constants are chosen within the constraints of microscopic reversibility, on the assumption that endless circulation around loops does not occur (see Hondeghem and Katzung [1977],

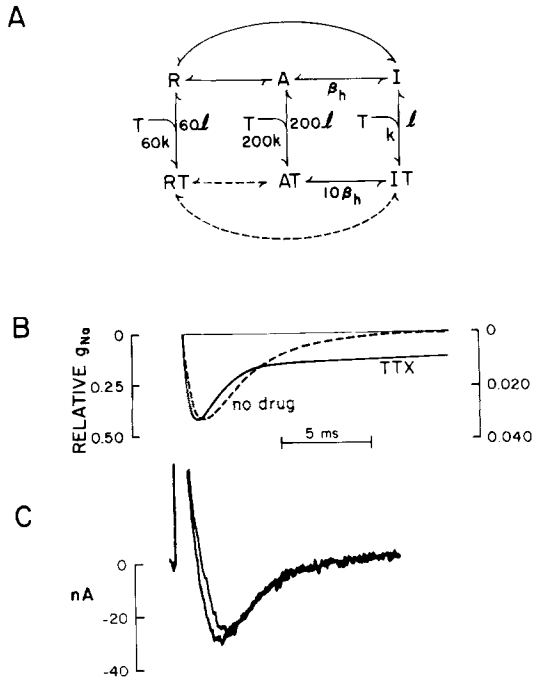

FIGURE 13. (A) Kinetic model for explaining the fast component of extra block in terms of rapid toxin binding to open channels. The model postulates that resting (R), activated (A), and inactivated (I) channels equilibrate with TTX at different speeds, and that bound toxin also affects speeds of gating reactions. Rate constants between R, A, and I were chosen to give a fairly realistic representation of sodium current in the absence of TTX (*B*, trace labeled *no drug*). Thus, in units of s^{-1}, $\kappa_{RA} = 495$, $\kappa_{AR} = 5$, $\kappa_{AI} = 199.8$, $\kappa_{IA} = 0.198$, $\kappa_{RI} = 199.8$, and $\kappa_{IR} = 0.002$. The remaining rate constants were adjusted to fit the family of data in Fig. 6 for 10 μM TTX. Onset and removal of extra block are governed by $\kappa_{I.IT} \equiv k = 1.53\ s^{-1}$, and $\kappa_{IT.I} \equiv \ell = 0.17\ s^{-1}$. Rates of toxin equilibration with R and A were speeded 60-fold and 200-fold, respectively. The factor of 200 was chosen to give a realistic amount of rapidly developing extra block; the factor of 60 was adjusted to give an almost monotonic recovery from extra block similar to that observed experimentally. Speeds of gating reactions among toxin-bound states were as follows: Transitions indicated by dashed lines were slowed 1,000-fold relative to corresponding reactions in the absence of toxin. The reaction between AT and IT was speeded 10-fold relative to the reaction between A and I. (B), calculated time-course of I_{Na} in the absence and presence of 10 μM toxin, using the parameters given in A. Vertical ordinates give sodium current as fraction of $\bar{g}_{Na}$. (*C*) experimental records of total membrane current in 0 TTX, 10 mM Na_o and 20 μM TTX, 40 mM Na_o evoked by a depolarizing step from −92 mV to −28 mV. Same vertical scale for both traces. There is a small increase in time-to-peak current in 20 μM TTX which was not consistently seen (cf. Fig. 1). Note that in TTX, I_{Na} decays no more rapidly and no less completely than in the absence of drug. Preparation C50-2, 17°C.

for a treatment that does not make this assumption). As in the four-state model, the state IT takes the role of the slowly recovering state, and recovery from block is attributed to the path IT → I → R. During a strong depolarization from a very negative holding potential, channels must transfer from the states R and RT to IT, as in Fig. 8. The fast phase of transfer cannot be RT → AT → IT, because this would not allow a sufficiently large amount of slowly developing extra block. Consequently, the transitions of toxin-bound channels from resting (RT) to either activated (AT) or inactivated (IT) states are taken to occur at extremely slow rates, as if the toxin molecule raised the activation energy barrier for these transitions. This is indicated by the *dashed arrows* in the figure. The two alternative pathways for the development of block are then

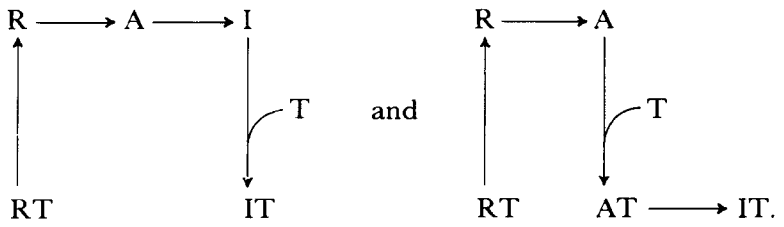

The pathway on the left is slow and associated with inactivation; that on the right is rapid and associated with activation. The latter pathway requires that TTX bind much more rapidly to activated channels than to either resting or inactivated channels, and also that AT → IT be faster than A → I. The parameter values indicated in Fig. 13*A* were chosen to satisfy these requirements and to fit the results in Fig. 6.

Set up in this way, the model predicts that TTX should alter the time-course of I_{Na}, much the same as those local anesthetics or other channel blockers that change the time-course of currents in other excitable membranes (Armstrong, 1969; Beam, 1976; Cahalan, 1978; Yeh and Narahashi, 1977). Fig. 13*B* shows calculations of normalized I_{Na} in 0 and 10 μM TTX. In the presence of toxin, the calculated decay is no longer a single exponential, but shows an initial decay that is faster than normal inactivation and a slower second component. The fast early decay arises because open channels can undergo not only inactivation (A → I) but also block (A → AT). The slower component arises because dissociation of toxin from RT provides a fresh supply of channels in R that can open and generate sodium current until RT is exhausted.

Unfortunately, these theoretical predictions are not borne out experimentally. Fig. 1 showed that the time-course of sodium current was not significantly changed by 1 or 4 μM TTX. We tested this point more rigorously by using very high TTX concentrations, increasing the external sodium concentration to compensate for tonic block. Fig. 13*C* shows that the decay phase is unaltered even by 20 μM TTX. Both records show the same monoexponential decay (τ_h = 4.3 ms). Closer examination of the data in TTX, out to the end of the 50-ms depolarization (not shown), failed to reveal a second exponential

component. These experimental results raise the question of how much leeway there is in the predictions of the model. The speeding of I_{Na} decay would not be seen if A → AT were negligible, but this would not allow enough rapidly developing block (25–40% in 20 ms in Figs. 11 and 12). Alternatively, the speeding of I_{Na} decay would not be evident if A ↔ AT were to reach equilibrium during the rising phase of I_{Na}. However, this would require a binding rate coefficient of the order of 10^9 $M^{-1}s^{-1}$, at least an order of magnitude faster than found for channel blocking drugs in other systems. Turning to the matter of the second exponential component, the constraints are even more severe. The slow component would become small enough to escape notice if RT → R equilibrated very slowly (e.g., $\tau \sim 100$ ms), but this would restrict the amount of rapidly developing extra block to less than the fraction initially in R. For 10 μM TTX, this limit would be 10%, far less than the 25–40% found in Figs. 11 and 12. Alternatively, if RT → R were very fast, the slow component would be abolished, but there could be little tonic block because channels in RT would be part of the pool available for activation.

These kinetic considerations, and difficulties of explaining how the saturating level of extra block varies with toxin concentration (p. 399), led us to consider a very different kind of model.

Rapidly Developing Extra Block as a Transition between Toxin-bound States

Fig. 14 shows a kinetic model that can account for all of the experimental observations. There are two new features. First, the normal sodium channel has two inactivated states, I1 and I2, as seems to be the case in nerve (Chiu, 1977; Armstrong and Bezanilla, 1977; see also Nonner [1980]). I1 and I2 are not strictly sequential (cf. Chiu, 1977) but can be reached via alternate branches from a common fork (see Armstrong and Bezanilla [1977]). Here, the fork is assumed to occur at state A. Second, the fast phase of extra block is attributed to interconversion between toxin-bound states, rather than to the binding of free toxin to open channels, as considered above. However, the basic principle is still that introduced in Fig. 8: extra block is accounted for by a toxin-bound inactivated state, I2T. As in the simpler kinetic schemes, TTX binds to all states of the channel with the same affinity, but not at the same rate. In this case, we postulate that the toxin equilibrates with I2 much more slowly (seconds) than with R, A, or I1 (within hundreds of milliseconds). Communication with I2T is further limited by the absence of the transitions RT ↔ I2T and I2T ↔ I1T, as if bound toxin greatly raised the activation energy for these reactions. All other transitions between toxin-bound states are assumed to be unaffected by the presence of bound TTX. Thus, I2T is assigned the role of the slowly recovering state.

The behavior of the model is illustrated in Fig. 14*b–d*. In a high TTX concentration, starting at a strongly negative resting potential, channels are distributed between R and RT, with most in RT. Fig. 14*b* shows how extra block develops for a weak depolarization. Channels in RT lose toxin to form R, and inactivate to form I2. They can then bind toxin to form I2T, or they can convert to I1 and then bind toxin to form I1T. Thus, the mechanism for

extra block during weak depolarizations is like that in Fig. 8 or Fig. 13, except that channels partition between a slowly recovering state (I2T) and a more rapidly repriming state (I1T). This partitioning can explain the failure of the saturating level of extra block to follow the simple one-to-one binding curve. An equilibrium distribution between I2:I1 (and I2T:I1T) of ~9:1 or 8:1

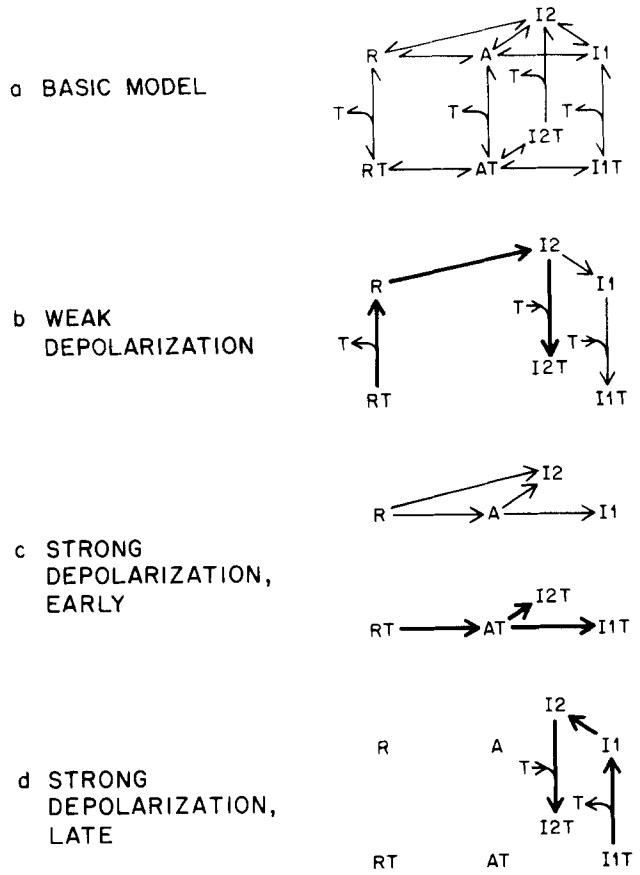

FIGURE 14. Kinetic interpretation of extra block and its inactivation-related and activation-related components. Rapidly developing extra block is attributed to transitions among toxin-blocked states. (*b–d*) The bold →, pathways that are crucial to determining the degree of extra block; →, other transitions occurring at the same time. The simple scheme in Fig. 8 corresponds to one facet of this model, indicated in *b* by →. For further details, see text.

would account for the saturating level of extra block in 1 and 10 μM TTX (Fig. 10).

Fig. 14*c* illustrates how rapid development of extra block might occur during a strong depolarization that clearly opens sodium channels. As the *heavy arrows* indicate, channels starting in RT first activate (AT), and then divide between I2T and I1T. The formation of I2T—extra block—shows a

voltage and time dependence similar to that of channel openness. However, because all the toxin-binding reactions are assumed to be slow relative to the rates of transition between toxin-free states, the development of extra block has little influence on the time-course of I_{Na} itself, as found in Fig. 13*C*. The scheme also provides an explanation for why the correlation between channel opening and rapidly developing extra block might be imperfect at moderate depolarizations where activation of channels is incomplete but where inactivation is complete. Toxin-free channels can inactivate directly, from R to I2, as well as through A, whereas toxin-bound channels must pass through AT. Thus, the occupancy of AT is only roughly mirrored by the number of open channels in state A. The measurement of sodium current would be an underestimate, particularly at weak depolarizations where the rate of inactivation (R → I2) is most comparable to the rate of activation (R → A). Thus, the prediction of the model is in qualitative agreement with Fig. 12.

After the first 10 or 20 ms of the depolarization, the fast phase of extra block gives way to a slower phase. The *heavy arrows* in Fig. 14*d* show how the slow phase can arise. Channels in I1T, which were initially protected from rapidly developing extra block, undergo a slower equilibrium with I2T by the pathway I1T → I1 → I2 → I2T. Because the last step is postulated to be much slower than the others, the overall rate will depend rather strongly on toxin concentration, as found experimentally for the slow phase of extra block (Fig. 10).

The branched topology of the model is significant: the fork at AT allows a balance between fast and slow components of extra block at various toxin concentrations. Fig. 10 shows that at 1 and 10 μM TTX, fast and slow components contribute roughly equal shares to total extra block if allowance is made for some recovery from extra block during the 1-s interpulse interval. This would be consistent with similar rates of transition from A → I1 and from A → I2. In the simpler six-state scheme, a fork between fast and slow paths to extra block is achieved, but only by invoking rapid toxin-binding to open channels (A → AT). Using the same kinetic framework, the combination of rapid and slow components cannot be accounted for by reactions between the three toxin-bound states because they do not form a "Y".

In summary, a kinetic model involving two inactivated states can account for a number of features of extra TTX block that are difficult to explain by simpler schemes: first, the lack of detectable change in I_{Na} time-course; second, the toxin dependence of extra block during long pulses; third, the relative apportionment of extra block into rapid and slow components. Quantitative modeling will be particularly useful as more information becomes available about the kinetic behavior of cardiac sodium channels in the absence of drug.

The analysis up to this point already raises some interesting issues for future experiments in heart and other excitable tissues. For example, measurements of Na channel gating current in the heart are needed to see if the "on" gating current associated with I_{Na} activation is strongly influenced by TTX, as Fig. 13 requires, or is relatively unaffected, as Fig. 14 predicts and as is found in nerve axons (Armstrong and Bezanilla, 1974; Neumcke et al., 1976). Previous

experiments indicate that nerve and skeletal muscle lack fast, activation-linked extra block, but leave open the question of whether inactivation-related extra block occurs during long-lasting potential changes on the time scale (minutes) of TTX binding and dissociation. How different are TTX and antiarrhythmic drugs such as lidocaine in their actions on cardiac sodium channels? Can the extra block produced by tertiary amine anesthetics be divided into activation- and inactivation-related components? Kinetic analysis along the lines of research presented in this paper may help explain how antiarrhythmic drugs act on cardiac impulses of different action potential configuration and frequency.

We thank Paul R. Adams and Roger Y. Tsien for helpful comments on the manuscript. This work was supported by U. S. Public Health Service grant HL 13306.

Received for publication 20 October 1980.

REFERENCES

ADAMS, P. R. 1976. Drug blockade of open end-plate channels. *J. Physiol (Lond.)*. **260:**531–552.

ALMERS, W., and S. R. LEVINSON. 1975. Tetrodotoxin binding to normal and depolarized frog muscle and the conductance of a single sodium channel. *J. Physiol. (Lond.)*. **247:**483–509.

ARMSTRONG, C. M. 1969. Inactivation of the potassium conductance and related phenomena caused by quaternary ammonium ion injection in squid axons. *J. Gen. Physiol.* **54:**553–575.

ARMSTRONG, C. M., and F. BEZANILLA. 1974. Charge movement associated with the opening and closing of the activation gates of the Na channels. *J. Gen. Physiol.* **63:**533–552.

ARMSTRONG, C. M., and F. BEZANILLA. 1977. Inactivation of the sodium channel. II. Gating current experiments. *J. Gen. Physiol.* **70:**567–590.

BAER, M., P. M. BEST, and H. REUTER. 1976. Voltage-dependent action of tetrodotoxin in mammalian cardiac muscle. *Nature (Lond.)*. **263:**344–345.

BEAM, K. G. 1976. A voltage clamp study of the effect of two lidocaine derivatives on the time course of end-plate currents. *J. Physiol. (Lond.)*. **258:**279–300.

BEAN, B. P., C. J. COHEN, T. J. COLATSKY, and R, W. TSIEN. 1980. Concentration-dependence of tetrodotoxin action on sodium currents and maximal upstroke velocity in rabbit cardiac Purkinje fibres. *J. Physiol. (Lond.)*. **305:**23P. (Abstr.).

BEAN, B. P., C. J. COHEN, and R. W. TSIEN. 1981. Lidocaine binding to resting and inactivated cardiac sodium channels. *Biophys. J.* **33:**208a. (Abstr.).

BROWN, A. M., W. GILES, J. R. HUME, and K. S. LEE. 1980. Voltage clamp analysis of lidocaine and quinidine induced depression of the sodium current in isolated rat ventricular cells. *J. Physiol. (Lond.)*. **307:**62P–63P. (Abstr.).

CALAHAN, M. D. 1978. Local anesthetic block of sodium channels in normal and pronase-treated squid giant axons. *Biophys. J.* **23:**285–311.

CALAHAN, M. D., and W. ALMERS. 1979. Interactions between quaternary lidocaine, the sodium channel gates, and tetrodotoxin. *Biophys. J.* **27:**39–55.

CARMELIET, E., and J. VEREECKE. 1969. Adrenaline and the plateau phase of the cardiac action potential. *Pfluegers Arch. Eur. J. Physiol.* **313:**300–315.

CHEN, C.-M., L. S. GETTES, and B. G. KATZUNG. 1975. Effect of lidocaine and quinidine on steady-state characteristics and recovery kinetics of $(dV/dt)_{max}$ in guinea pig ventricular myocardium. *Circ. Res.* **37:**20–29.

CHIU, S. Y. 1977. Inactivation of sodium channels: second order kinetics in myelinated nerve. *J. Physiol. (Lond.)*. **273:**573–596.

COHEN, C. J. B. P. BEAN, and R. W. TSIEN. 1981. Block of cardiac sodium channels by TTX and lidocaine: sodium current and $\dot{V}_{max}$ experiments. *In* Normal and Abnormal Conduction in the Heart. B. F. Hoffman, M. Lieberman, and A. Paes de Carvalho, editors. Futura Publishing Co., Inc., Mt. Kisco, N. Y. In press.

COHEN, C. J., T. J. COLATSKY, and R. W. TSIEN. 1979. Tetrodotoxin block of cardiac sodium channels during repetitive or steady depolarization. *J. Physiol. (Lond.)*. **296:**70P. (Abstr.).

COHEN, I. S., and G. R. STRICHARTZ. 1977. On the voltage dependent action of tetrodotoxin. *Biophys. J.* **17:**275–279.

COHEN, I. S., D. ATTWELL, and G. R. STRICHARTZ. 1981. The dependence of the maximal rate of rise of the action potential upstroke on membrane properties. *Proc. R. Soc. Lond. B Biol. Sci.* In press.

COLATSKY, T. J. 1980. Voltage clamp measurements of sodium channel properties in rabbit cardiac Purkinje fibres. *J. Physiol. (Lond.)*. **305:**215–234.

COLATSKY, T. J., and D. C. GADSBY. 1980. Is tetrodotoxin block of background sodium channels in cardiac Purkinje fibres voltage-dependent? *J. Physiol. (Lond.)*. **306:**20P. (Abstr.).

COLATSKY, T. J., and R. W. TSIEN. 1979. Sodium channels in rabbit cardiac Purkinje fibres. *Nature (Lond.)*. **278:**265–268.

COLQUHOUN, D. 1971. Lectures on Biostatistics. Oxford University Press, Oxford. London.

COLQUHOUN, D., R. HENDERSON, and J. M. RITCHIE. 1972. The binding of labelled tetrodotoxin to non-myelinated nerve fibres. *J. Physiol. (Lond.)*. **227:**95–126.

COLQUHOUN, D., H. P. RANG, and J. M. RITCHIE. 1974. The binding of tetrodotoxin and α-bungarotoxin to normal and denervated mammalian muscle. *J. Physiol. (Lond.)*. **240:**199–226.

CORABOEUF, E., E. DEROUBAIX, and A. COULOMBE. 1979. Effect of tetrodotoxin on action potentials of the conducting system in the dog heart. *Am. J. Physiol.* **237:**H561–H567.

COURTNEY, K. 1974. Frequency-dependent inhibition of sodium currents in frog myelineated nerve by GEA 968, a new lidocaine derivative. Ph.D. Thesis. University of Washington, Seattle, Wash. (Available from University Microfilms, Ann Arbor, Mich.; No. 74-29, 393.)

COURTNEY, K. R. 1975. Mechanism of frequency-dependent inhibition of sodium currents in frog myelinated nerve by the lidocaine derivative GEA 968. *J. Pharmacol. Exp. Ther.* **195:** 225–236.

DUDEL, J., K. PEPER, R. RÜDEL, and W. TRAUTWEIN. 1967. The effect of tetrodotoxin on the membrane current in cardiac muscle (Purkinje fibers). *Pfluegers Arch. Eur. J. Physiol.* **295:** 213–226.

GAGE, P. W., J. W. MOORE, and M. WESTERFIELD. 1976. An octopus toxin, maculotoxin, selectively blocks sodium current in squid axons. *J. Physiol. (Lond.)*. **259:**427–443.

HARVEY, C., E. ROJAS, and B. A. SUAREZ-ISLA. 1979. Slow sodium conductance inactivation in frog skeletal muscle fibres. *J. Physiol. (Lond.)*. **291:**56P. (Abstr.).

HEISTRACHER, P. 1971. Mechanism of action of antifibrillatory drugs. *Naunyn-Schmiedebergs Arch. Pharmacol.* **269:**199–212.

HILLE, B. 1968. Pharmacological modifictions of the sodium channels of frog nerve. *J. Gen. Physiol.* **51:**199–219.

HILLE, B. 1970. Ionic channels in nerve membrane. *Prog. Biophys. Mol. Biol.* **21:**1–32.

HILLE, B. 1977. Local anesthetics: hydrophilic and hydrophobic pathways for the drug-receptor reaction. *J. Gen. Physiol.* **69:**497–515.

HILLE, B. 1978. Local anesthetic action on inactivation of the Na channel in nerve and skeletal muscle: possible mechanisms for antiarrhythmic agents. *In* Biophysical Aspects of Cardiac Muscle. M. Morad, editor. Academic Press, Inc., New York. 55–74.

HODGKIN, A. L., and A. F. HUXLEY. 1952. The dual effect of membrane potential on sodium conductance in the giant axon of *Loligo*. *J. Physiol.* (*Lond.*). **116:**497–506.

HOFFMAN, B. F., and P. F. CRANEFIELD. 1960. Electrophysiology of the Heart. McGraw-Hill, Inc., New York.

HONDEGHEM, L. M. 1978., Validity of $\dot{V}_{max}$ as a measure of the sodium current in cardiac and nervous tissues. *Biophys. J.* **23:**147–152.

HONDEGHEM, L. M., and B. G. KATZUNG. 1977. Time- and voltage-dependent interactions of antiarrhythmic drugs with cardiac sodium channels. *Biochim. Biophys. Acta.* **472:**373–398.

HUNTER, P. J., P. A. MCNAUGHTON, and D. NOBLE. 1975. Analytical models of propagation in excitable cells. *Prog. Biophys. Mol. Biol.* **30:**99–144.

JAIMOVICH, E., R. A. VENOSA, P. SHRAGER, and P. HOROWICZ. 1976. Density and distribution of tetrodotoxin receptors in normal and detubulated frog sartorius muscle. *J. Gen. Physiol.* **67:**399–416.

JOHNSON, E. A., and M. C. MCKINNON. 1957. The differential effect of quinidine and pyrilamine on the myocardial action potential at various rates of stimulation. *J. Pharmacol. Exp. Ther.* **120:**460–468.

KHODOROV, B. I., and V. I. BELYAYEV. 1967. Effect of membrane hyperpolarization and of calcium and nickel ions on electrical activity of the single node of Ranvier on exposure to tetrodotoxin and procaine. *Biophysics* (*Engl. Trans. Biofizika*). **12:**981–992.

KHODOROV, B., L. SHISHKOVA, E. PEGANOV, and S. REVENKO. 1976. Inhibition of sodium currents in frog Ranvier node treated with local anesthetics. Role of slow sodium inactivation. *Biochim. Biophys. Acta.* **433:**409–435.

KHODOROV, B. I., and E. N. TIMIN. 1975. Nerve impulse propagation along nonuniform fibres. *Prog. Biophys. Mol. Biol.* **30:**145–184.

MARY-RABINE, L., B. F. HOFFMAN, and M. R. ROSEN. 1979. Participation of slow inward current in the Purkinje fiber action potential overshoot. *Am. J. Physiol.* **237:**H204–H212.

MEVES, H. 1978. Inactivation of the sodium permeability in squid giant nerve fibres. *Prog. Biophys. Mol. Biol.* **33:**207–230.

NARAHASHI, T. 1974. Chemicals as tools in the study of excitable membranes. *Physiol. Rev.* **54:** 813–889.

NEHER, E., and J. H. STEINBACH. 1978. Local anesthetics transiently block currents through single acetylcholine-receptor channels. *J. Physiol.* (*Lond.*). **277:**153–176.

NEUMCKE, B., W. NONNER, and R. STÄMPFLI. 1976. Asymmetrical displacement current and its relation with the activation of sodium current in the membrane of frog myelinated nerve. *Pfluegers Arch. Eur. J. Physiol.* **363:**193–203.

NONNER, W. 1980. Relations between the inactivation of sodium channels and the immobilization of gating charge in frog myelinated nerve. *J. Physiol.* (*Lond.*). **299:**573–603.

PAPPONE, P. A. 1980. Voltage-clamp experiments in normal and denervated mammalian skeletal muscle fibres. *J. Physiol.* (*Lond.*). **306:**377–410.

REUTER, H., M. BAER, and P. M. BEST. 1978. Voltage dependence of TTX action in mammalian cardiac muscle. *In* Biophysical Aspects of Cardiac Muscle. M. Morad, editor. Academic Press, Inc., New York. 129–142.

RITCHIE, J. M., and R. B. ROGART. 1977. The binding of saxitoxin and tetrodotoxin to excitable tissue. *Rev. Physiol. Biochem. Pharmacol.* **79:**1–50.

ROBINSON, R. B., and W. W. SLEATOR. 1977. Tetrodotoxin effects in mammalian cardiac muscle: frequency and calcium dependence. *Proc. Int. Union Physiol. Sci.* **13:**632. (Abstr.)

RUFF, R. L. 1977. A quantitative analysis of local anesthetic alteration of miniature end-plate currents and end-plate current fluctuations. *J. Physiol. (Lond.)*. **264:**89–124.

SANO, T., F. SUZUKI, S. SATO, and Y. IIDA. 1968. Mode of action of new antiarrhythmic agents. *Jpn. Heart J.* **9:**161–168.

SCHOLZ, H. 1969. Ca-abhängige Membranpotentialänderungen am Herzen und ihre Bedeutung für die elektro-mechanische Kopplung. Versuche mit Tetrodotoxin in Na-haltigen Lösungen. *Naunyn-Schmiedebergs Arch. Pharmacol.* **265:**187–204.

SCHWARZ, W., P. T. PALADE, and B. HILLE. 1977. Local anesthetics. Effect of pH on use-dependent block of sodium channels in frog muscle. *Biophys. J.* **20:**343–368.

STAIMAN, A. L., and P. SEEMAN. 1975. Different sites of membrane action for tetrodotoxin and lipid-soluble anesthetics. *Can. J. Physiol. Pharmacol.* **53:**513–524.

STRICHARTZ, G. R. 1973. The inhibition of sodium currents in myelinated nerve by quaternary derivatives of lidocaine. *J. Gen. Physiol.* **62:**37–57.

STRICHARTZ, G., and I. COHEN. 1978. $\dot{V}_{max}$ as a measure of $\bar{G}_{Na}$ in nerve and cardiac membranes. *Biophys. J.* **23:**153–156.

TAKATA, M., J. W. MOORE, C. Y. KAO, and F. A. FURHMAN. 1966. Blockage of sodium conductance increase in lobster giant axon by tarichatoxin (tetrodotoxin). *J. Gen. Physiol.* **49:**977–988.

ULBRICHT, W. 1977. Ionic channels and gating currents in excitable membranes. *Annu. Rev. Biophys. Bioeng.* **6:**7–31.

ULBRICHT, W., and H.-H. WAGNER. 1975. The influence of pH on equilibrium effects of tetrodotoxin on myelinated nerve fibres of *Rana esculenta*. *J. Physiol. (Lond.)*. **252:**159–184.

WAGNER, H.-H., and W. ULBRICHT. 1976. Saxitoxin and procaine act independently on separate sites of the sodium channel. *Pfluegers Arch. Eur. J. Physiol.* **364:**65–70.

WALTON, M., and H. A. FOZZARD. 1979. The relation of V_{max} to I_{Na}, G_{Na}, and h_∞ in a model of cardiac Purkinje fiber. *Biophys. J.* **25:**407–420.

WEIDMANN, S. 1955*a*. The effect of the cardiac membrane potential on the rapid availability of the sodium carrying system. *J. Physiol. (Lond.)*. **127:**213–224.

WEIDMANN, S. 1955*b*. The effects of calcium ions and local anesthetics on electrical properties of Purkinje fibres. *J. Physiol. (Lond.)*. **129:**568–582.

YANAGA, T., and W. C. HOLLAND. 1970. Effect of tetrodotoxin on transmembrane potential of atrial muscle. *J. Pharmacol. Exp. Ther.* **171:**20–25.

YEH, J. Z., and C. M. ARMSTRONG. 1978. Immobilization of gating charge by a substance that simulates inactivation. *Nature (Lond.)*. **273:**387–389.

YEH, J. Z., and T. NARAHASHI. 1977. Kinetic analysis of pancuronium interaction with sodium channels in squid axon membranes. *J. Gen. Physiol.* **69:**293–323.